第 29 卷 第 8 期 材 料 研 究 学 报 Vol. 29 No. 8
2 0 1 5 年 8 月 CHINESE JOURNAL OF MATERIALS RESEARCH August 2 0 1 5

聚苯胺-钴铬锌铁氧体复合材料的微波吸收性能和磁性能*

马瑞廷 蒋 丹 王 晓 赵海涛

(沈阳理工大学材料科学与工程学院 沈阳 110159)

摘 要 用聚丙烯酰胺凝胶法和原位聚合法分别制备了钴铬锌铁氧体($Co_{0.7}Cr_{0.1}Zn_{0.2}Fe_2O_4$)和聚苯胺-钴铬锌铁氧体复合材料(PANI-$Co_{0.7}Cr_{0.1}Zn_{0.2}Fe_2O_4$), 用XRD和FT-IR对材料的结构进行了表征。结果表明, 制备的$Co_{0.7}Cr_{0.1}Zn_{0.2}Fe_2O_4$铁氧体为尖晶石结构, 少量$Cr^{3+}$离子替代了铁氧体八面体位置上的$Co^{2+}$离子, 导致铁氧体的晶格常数从0.8409 nm减小到0.8377 nm。用振动样品磁强计(VSM)测量了材料的磁性能, 结果表明, PANI-$Co_{0.7}Cr_{0.1}Zn_{0.2}Fe_2O_4$复合材料的饱和磁化强度($M_s$)、剩余磁化强度($M_r$)和矫顽力($H_c$)分别为8.80 emu/g、14 emu/g和37.22 kA/m, 小于铁氧体的相应数值; 用波导法研究了PANI-$Co_{0.7}Cr_{0.1}Zn_{0.2}Fe_2O_4$复合材料的微波吸收性能, 在5−20 GHz频率范围内14.1 GHz和17.9 GHz处出现两个极大反射损耗, 分别为−13.17 dB和−15.36 dB, 大于铁氧体的反射损耗。

关键词 复合材料, 铁氧体, 聚苯胺, 微波吸收性能, 磁性能

分类号 O646, O614 文章编号 1005-3093(2015)08-0622-05

Microwave Absorbing and Magnetic Properties of the Polyaniline-$Co_{0.7}Cr_{0.1}Zn_{0.2}Fe_2O_4$ Composites

MA Ruiting** JIANG Dan WANG Xiao ZHAO Haitao

(School of Materials Science and Engineering, Shenyang Ligong University, Shenyang 110159, China)

Supported by National Science Foundation of Liaoning Province No.2014020094.

Manuscript received November 27, 2014; in revised form December 18, 2014.

To whom correspondence should be addressed, Tel: 13840421062, E-mail: mrt-1118@163.com

ABSTRACT The spinel cobalt chromium zinc ferrites ($Co_{0.7}Cr_{0.1}Zn_{0.2}Fe_2O_4$) and composites of polyaniline (PANI)-$Co_{0.7}Cr_{0.1}Zn_{0.2}Fe_2O_4$ were prepared by polyacrylamide gel and *in situ* polymerization method, respectively, and then the synthesized materials were characterized by X-ray diffraction (XRD) and Fourier transform infrared spectrometer (FT-IR), their magnetic properties were measured using vibrating sample magnetometer (VSM) and their microwave absorbing capability was investigated by wave-guide method. The results show that the spinel $Co_{0.7}Cr_{0.1}Zn_{0.2}Fe_2O_4$ ferrites and the composites PANI-$Co_{0.7}Cr_{0.1}Zn_{0.2}Fe_2O_4$ are acquired. Because a small amount Co^{2+} ion of the octahedron ferrite is replaced by Cr^{3+} ions, the lattice constant of the $Co_{0.8}Zn_{0.2}Fe_2O_4$ ferrite reduces from 0.8409 nm to 0.8377 nm. The saturation magnetization (M_s), remanent magnetization (M_r) and coercive force (H_c) of the PPy-$Co_{0.7}Cr_{0.1}Zn_{0.2}Fe_2O_4$ composites are 8.80 emu·g^{-1}, 3.14 emu·g^{-1} and 37.22 kA·m^{-1}, respectively, which are smaller than that of the $Co_{0.7}Cr_{0.1}Zn_{0.2}Fe_2O_4$ ferrite. In a measuring frequency range of 5.0-20.0 GHz, two peak values of reflection loss for the composites PPy-$Co_{0.7}Cr_{0.1}Zn_{0.2}Fe_2O_4$ appear at 14.1 GHz and 17.9 GHz with -13.17 dB and -15.36 dB, respectively, which is obviously higher than those of the $Co_{0.7}Cr_{0.1}Zn_{0.2}Fe_2O_4$ ferrite.

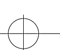
KEY WORDS composites, ferrite, polyaniline, microwave absorbing properties, magnetic properties

各种电子设备产生的电磁辐射和电磁干扰, 给人们的生活带来了严重的影响。因此, 对吸波材料的研究迫在眉睫。尖晶石型铁氧体(MFe_2O_4, M=Fe, Co, Ni, Zn等)具有化学稳定性好、吸收性能高、吸波频带宽、价格低廉以及涂层薄等优点, 是备受关注的电磁屏蔽材料[1]。Sun等[2]用固相法制备了MnZn铁氧体, 并研究了铁氧体的磁损耗(P_L)随温度的变化; 吴燕飞等[3]用溶胶-凝胶法制备Me_2-W型铁氧体($BaMe_2Fe_{16}O_{27}$), 并考察了Co^{2+}、Ni^{2+}、Zn^{2+}作为Me_2组合时电磁性能的变化。但是, 铁氧体吸波材料的介

* 辽宁省自然科学基金2014020094和沈阳市重点实验室建设基金F14-187-1-00资助项目。

2014年11月27日收到初稿; 2014年12月18日收到修改稿。

本文联系人: 马瑞廷



电损耗小和面密度大等缺点限制了其使用范围。介电型吸波材料聚苯胺具有质量轻、抗腐蚀性强和环境稳定性高等优点而受到研究人员的重视, 但因其磁损耗几乎为零使其难以作为单一的吸波材料使用[4,5]。

聚合物/铁氧体复合材料在两相界面上产生协同效应, 使复合材料兼具聚合物和铁氧体的特性, 越来越受到材料工作者的重视[6-8]。李元勋等[6]用原位掺杂法将聚苯胺包覆到M型钡铁氧体粒子表面, 使其反射率小于−20 dB时频带宽达到15.07 GHz。Gairola[7]等用机械共混法合成PANI-$Mn_{0.2}Ni_{0.4}Zn_{0.4}Fe_2O_4$复合材料, 并研究了涂覆厚度对复合材料的电磁屏蔽性能的影响。Yang等[8]用原位聚合法制备的PANI-$BaFe_{12}O_{19}$复合材料, 在2.0−26.5 GHz频率范围内其存在两个吸收频带, 在7.8 GHz和24.2 GHz处有极大的反射损耗, 分别为−12.5 dB和−11.5 dB。本文采用原位聚合法制备PANI-$Co_{0.7}Cr_{0.1}Zn_{0.2}Fe_2O_4$复合材料, 并研究其结构、介电损耗、反射损耗和磁性能。

1 实验方法

1.1 样品的制备

用聚丙烯酰胺凝胶法制备$Co_{0.7}Cr_{0.1}Zn_{0.2}Fe_2O_4$铁氧体[9], 用原位聚合法制备Polyaniline-$Co_{0.7}Cr_{0.1}Zn_{0.2}Fe_2O_4$复合材料。将1.86 g已蒸馏的苯胺(an)单体, 3.44 g十二烷基苯磺酸(DBSA)、0.186 g $Co_{0.7}Cr_{0.1}Zn_{0.2}Fe_2O_4$铁氧体和100 mL蒸馏水加到三口烧瓶中, 超声搅拌1 h后加入大量冰块降温; 待温度降至0℃左右时用恒压滴液漏斗将100 mL溶解有4.56 g过硫酸铵(APS)的蒸馏水匀速滴加到反应体系中, (在30 min内)滴完后继续聚合反应8 h, 在此过程中不断向其中加入冰块以保证整个聚合反应温度保持着0℃左右。将三口烧瓶中的反应物转入500 mL烧杯中, 加入200 mL丙酮破乳后静置24 h, 抽滤后将滤饼用无水乙醇和蒸馏水反复洗涤, 滤液为无色透明后将滤饼在60℃下真空干燥3 h。所得墨绿色粉末, 即为PANI-$Co_{0.7}Cr_{0.1}Zn_{0.2}Fe_2O_4$复合材料。

1.2 样品的表征

用D/max-RB型X射线衍射仪分析产物的物相组成(CuK_α辐射, 靶电压: 40 kV, 靶电流: 100 mA。采用q-2q步进扫描方式, 步长0.02°, 扫描速率7°/min)。用傅里叶变换红外光谱仪(AVATAR-360, FT-IR)分析样品的红外吸收峰。用VSM-220振动样品磁强计测定产物的饱和磁化强度M_s、剩余磁化强度M_r和矫顽力H_c(施加的最大磁场为20 kOe)。用波导法使用E5071C矢量网络分析仪测试样品的介电常数和反射损耗。

2 结果和讨论

2.1 XRD 分析

图1分别给出了PANI-$Co_{0.7}Cr_{0.1}Zn_{0.2}Fe_2O_4$, $Co_{0.7}Cr_{0.1}Zn_{0.2}Fe_2O_4$和$Co_{0.8}Zn_{0.2}Fe_2O_4$的XRD谱。由图1c可以看出, $Co_{0.8}Zn_{0.2}Fe_2O_4$的谱线在2θ=18.18°、30.08°、35.40°、43.04°、53.40°、56.90°、62.42°处均出现了具有立方晶系尖晶石结构的特征衍射峰, 分别对应(111)、(220)、(311)、(400)、(422)、(511)、(440)晶面, 与尖晶石结构的$Co_{0.8}Zn_{0.2}Fe_2O_4$(JCPDS卡号22-1086)的特征衍射峰一致, 表明所得产物为尖晶石结构的$Co_{0.8}Zn_{0.2}Fe_2O_4$铁氧体。

与图1c比较, 图1b所有衍射峰的位置均略微右移, 但没有改变$Co_{0.8}Zn_{0.2}Fe_2O_4$的晶型。这说明Cr^{3+}取代了Co^{2+}进入到$Co_{0.8}Zn_{0.2}Fe_2O_4$铁氧体的晶格中, 即成功合成了$Co_{0.7}Cr_{0.1}Zn_{0.2}Fe_2O_4$。从图1b和c可以看出, $Co_{0.8}Zn_{0.2}Fe_2O_4$的(311)晶面位置为35.40°, $Co_{0.7}Cr_{0.1}Zn_{0.2}Fe_2O_4$铁氧体(311)晶面位置为35.54°, 其晶格常数可用如下公式计算[10]

$$\alpha = \frac{\lambda(h^2+k^2+l^2)}{2\sin\theta}$$

式中α为晶格常数, λ为X射线的波长(这里为0.154178 nm), (hkl)为最强峰对应的(311)晶面的晶面指数。计算结果: $Co_{0.8}Zn_{0.2}Fe_2O_4$的晶格常数为0.8409 nm, 大于$Co_{0.7}Cr_{0.1}Zn_{0.2}Fe_2O_4$的晶格常数0.8377 nm。当$Cr^{3+}$离子进入$Co_{0.8}Zn_{0.2}Fe_2O_4$铁氧体晶格时, 处于八面体位置上的少量$Co^{2+}$被$Cr^{3+}$取代。$Cr^{3+}$离子的有效半径为0.0615 nm, 小于$Co^{2+}$离子的

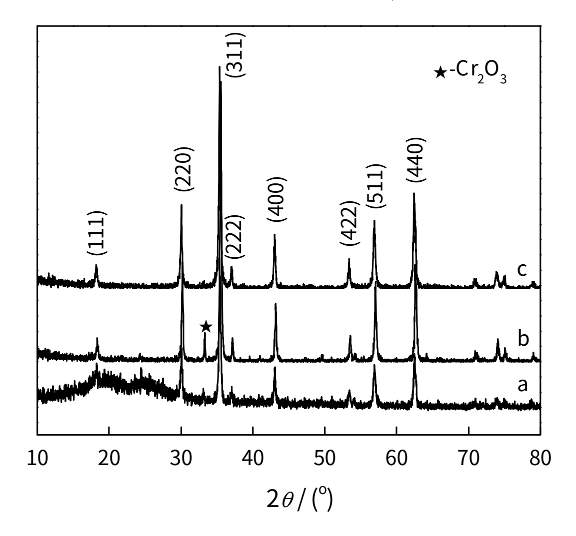


图1 PANI-$Co_{0.7}Cr_{0.1}Zn_{0.2}Fe_2O_4$, $Co_{0.7}Cr_{0.1}Zn_{0.2}Fe_2O_4$和$Co_{0.8}Zn_{0.2}Fe_2O_4$的XRD谱

Fig.1 XRD spectra of the samples, (a) PANI-$Co_{0.7}Cr_{0.1}Zn_{0.2}Fe_2O_4$, (b) $Co_{0.7}Cr_{0.1}Zn_{0.2}Fe_2O_4$ and (c) $Co_{0.8}Zn_{0.2}Fe_2O_4$

有效半径0.0745 nm, 因此$Co_{0.7}Cr_{0.1}Zn_{0.2}Fe_2O_4$的晶格常数减小, 在XRD谱上的表现为$Co_{0.7}Cr_{0.1}Zn_{0.2}$-$Fe_2O_4$的衍射峰的位置发生轻微右移; 此外, 在图1b的2θ=33.30°处出现了杂质峰, 为Cr_2O_3的衍射峰。在图1a中不仅出现了$Co_{0.7}Cr_{0.1}Zn_{0.2}Fe_2O_4$的特征峰, 在2$\theta$=19.8°和25.6°处还出现了两处宽泛的衍射峰。这是本征态PANI的衍射峰, 聚苯胺分子链中含有大量刚性苯环, 使聚苯胺具有周期性平行和垂直的性质, 并有一定的结晶度, 因而其XRD谱发生散射形成了较为宽泛的衍射花样[11, 12], 表明所得产物为PANI-$Co_{0.7}Cr_{0.1}Zn_{0.2}Fe_2O_4$复合材料。

2.2 FT-IR分析

图2a和b分别给出了PANI-$Co_{0.7}Cr_{0.1}Zn_{0.2}Fe_2O_4$和$Co_{0.7}Cr_{0.1}Zn_{0.2}Fe_2O_4$的红外光谱图。图2b中在波数为572 cm^{-1}处有一明显的吸收峰, 对应铁氧体中金属离子与氧离子(M-O)之间的伸缩振动吸收峰, 属于V_1振动吸收峰, 为尖晶石型铁氧体结构中四面体的特征振动吸收[13]。由图2a可以看出, 波数在3446 cm^{-1}和1387 cm^{-1}处的吸收峰为聚苯胺中N—H键的伸缩振动吸收峰; 在1566 cm^{-1}和1491 cm^{-1}处的吸收峰对应着苯环和醌环的C=C双键的伸缩振动; 1237 cm^{-1}处的吸收峰为聚苯胺长链上C—N键的伸缩振动; 在1116 cm^{-1}处出现的强吸收峰为N=Q=N(Q表示醌环)的振动吸收峰[14, 15], 表明所得产物中含有聚苯胺; 同时图2a中在572 cm^{-1}处也出现了铁氧体中M—O键的特征伸缩振动吸收峰, 但是强度有所减弱, 表明合成了PANI-$Co_{0.7}Cr_{0.1}Zn_{0.2}Fe_2O_4$复合材料。这与X-ray衍射结果是一致的。

2.3 磁性能

图3a和b分别给出了PANI-$Co_{0.7}Cr_{0.1}Zn_{0.2}Fe_2O_4$和$Co_{0.7}Cr_{0.1}Zn_{0.2}Fe_2O_4$的磁滞回线图。从图中可得到各物质的饱和磁化强度$M_s$、剩余磁化强度$M_r$和矫顽力$H_c$等磁性参数, 列于表1。从表1可见, PANI-$Co_{0.7}Cr_{0.1}Zn_{0.2}Fe_2O_4$复合材料的$M_s$和$M_r$的值分别为8.80 emu·$g^{-1}$和3.14 emu·$g^{-1}$, 小于铁氧体的$M_s$=73.84 emu·$g^{-1}$和$M_r$=28.43 emu·$g^{-1}$, 但是$H_c$为37.22 kA·$m^{-1}$, 略小于$Co_{0.7}Cr_{0.1}Zn_{0.2}Fe_2O_4$的38.91 kA·$m^{-1}$。$Co_{0.7}Cr_{0.1}$-$Zn_{0.2}Fe_2O_4$铁氧体属于磁损耗型介质。根据电磁学理论, 铁氧体的磁性主要取决于铁原子未填满的3d电子层的电子磁矩, 未成对的d电子越多, 磁矩μ则越大; 而聚苯胺属于电损耗型介质, 几乎没有磁性能。PANI-$Co_{0.7}Cr_{0.1}Zn_{0.2}Fe_2O_4$复合材料的磁性主要来源于铁氧体, 因而掺杂后PANI-$Co_{0.7}Cr_{0.1}$-$Zn_{0.2}Fe_2O_4$复合材料的磁性参数都小于铁氧体的。

2.4 介电损耗

在测试频率范围(5−20 GHz)内PANI-$Co_{0.7}Cr_{0.1}$-$Zn_{0.2}Fe_2O_4$ (a)和$Co_{0.7}Cr_{0.1}Zn_{0.2}Fe_2O_4$ (b)的介电损耗($\tan\varepsilon=\varepsilon''/\varepsilon'$)随测试频率变化曲线, 如图4所示。由图4可见, 在测试频率范围内, PANI-$Co_{0.7}Cr_{0.1}Zn_{0.2}Fe_2O_4$复合材料的$\tan\varepsilon$在0.67−0.80之间明显高于$Co_{0.7}Cr_{0.1}Zn_{0.2}Fe_2O_4$的$\tan\varepsilon$在0.10−0.36之间。介电损耗主要取决于材料内部电偶极子的极化作用[16]。根

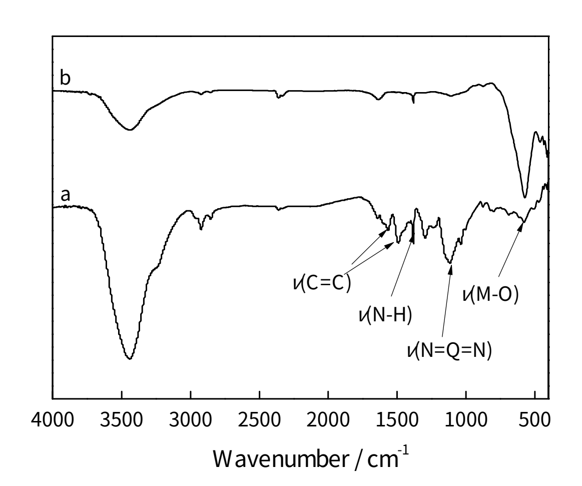


图2 PANI-$Co_{0.7}Cr_{0.1}Zn_{0.2}Fe_2O_4$和$Co_{0.7}Cr_{0.1}Zn_{0.2}Fe_2O_4$的红外光谱图

Fig.2 FT-IR spectra of the samples (a) PANI-$Co_{0.7}Cr_{0.1}$-$Zn_{0.2}Fe_2O_4$, (b) $Co_{0.7}Cr_{0.1}Zn_{0.2}Fe_2O_4$

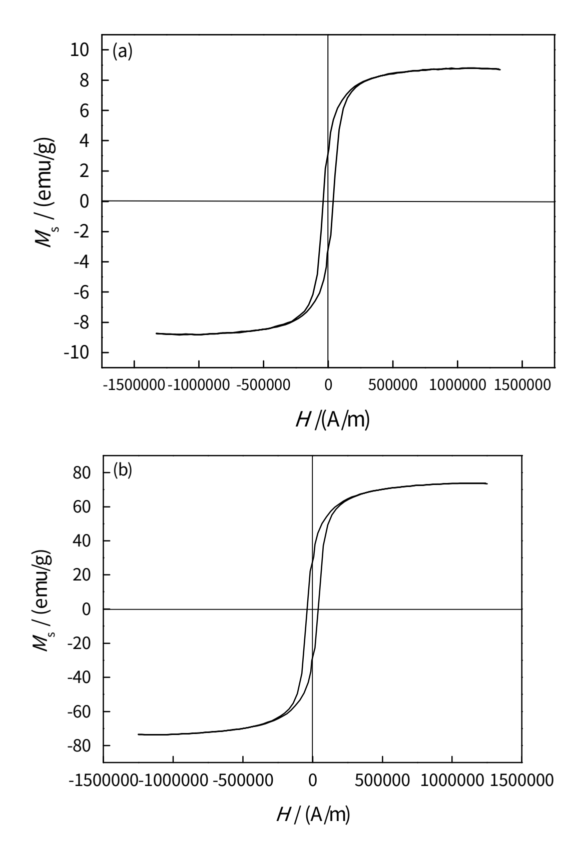


图3 PANI-$Co_{0.7}Cr_{0.1}Zn_{0.2}Fe_2O_4$和$Co_{0.7}Cr_{0.1}Zn_{0.2}Fe_2O_4$的磁滞回线图

Fig.3 Hysteresis loops of the samples (a) PANI-$Co_{0.7}Cr_{0.1}$-$Zn_{0.2}Fe_2O_4$, (b) $Co_{0.7}Cr_{0.1}Zn_{0.2}Fe_2O_4$

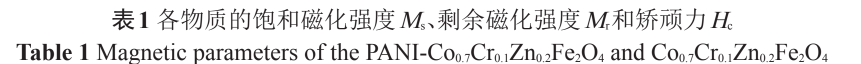


表 1 各物质的饱和磁化强度 M_s、剩余磁化强度 M_r 和矫顽力 H_c

Table 1 Magnetic parameters of the PANI-$Co_{0.7}Cr_{0.1}Zn_{0.2}Fe_2O_4$ and $Co_{0.7}Cr_{0.1}Zn_{0.2}Fe_2O_4$

Sample	Magnetic parameters		
	M_s	M_r	H_c
PANI-$Co_{0.7}Cr_{0.1}Zn_{0.2}Fe_2O_4$	8.80	3.14	37.22
$Co_{0.7}Cr_{0.1}Zn_{0.2}Fe_2O_4$	73.84	28.43	38.91

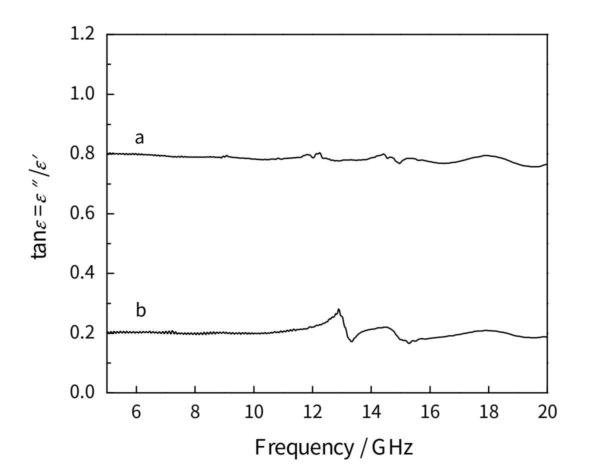


图 4 PANI-$Co_{0.7}Cr_{0.1}Zn_{0.2}Fe_2O_4$ 和 $Co_{0.7}Cr_{0.1}Zn_{0.2}Fe_2O_4$ 的介电损耗($\tan\varepsilon=\varepsilon''/\varepsilon'$)随频率的变化曲线

Fig.4 Dielectric loss curves of the samples, (a) PANI-$Co_{0.7}Cr_{0.1}Zn_{0.2}Fe_2O_4$, (b) $Co_{0.7}Cr_{0.1}Zn_{0.2}Fe_2O_4$

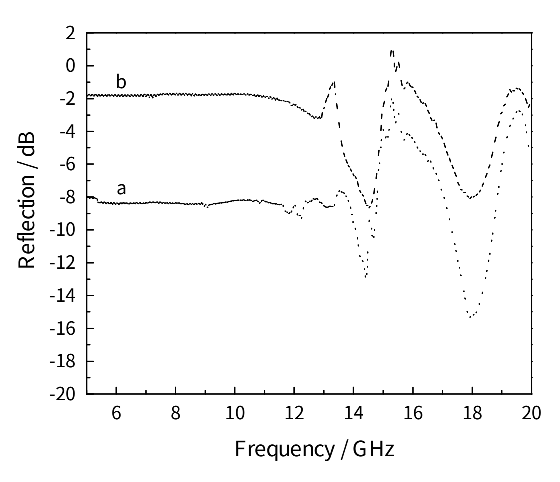


图 5 PANI-$Co_{0.7}Cr_{0.1}Zn_{0.2}Fe_2O_4$ 和 $Co_{0.7}Cr_{0.1}Zn_{0.2}Fe_2O_4$ 的反射损耗随频率的变化曲线

Fig.5 Reflection loss curves of the samples, (a) PANI-$Co_{0.7}Cr_{0.1}Zn_{0.2}Fe_2O_4$, (b) $Co_{0.7}Cr_{0.1}Zn_{0.2}Fe_2O_4$

据复介电常数理论, 当电磁波照射到介电材料表面时, 由于铁氧体颗粒表面与PANI大分子链之间存在相互作用[17], 在复合材料内部产生传导电流和位移电流, 引起介电松弛效应和空间电荷极化效应, 导致PANI-$Co_{0.7}Cr_{0.1}Zn_{0.2}Fe_2O_4$的介电损耗比单一的铁氧体大。同时, 铁氧体为磁损耗型吸波材料, 几乎不具有介电性能, 而PANI为介电损耗型吸波材料, 故当铁氧体颗粒被PANI包覆后其介电损耗增大。

2.5 反射损耗

PANI-$Co_{0.7}Cr_{0.1}Zn_{0.2}Fe_2O_4$ (a)和 $Co_{0.7}Cr_{0.1}Zn_{0.2}Fe_2O_4$ (b)的反射损耗随测试频率变化曲线, 如图5所示。在测试频率(5−20 GHz)范围内PANI-$Co_{0.7}Cr_{0.1}$-$Zn_{0.2}Fe_2O_4$复合材料在14.1 GHz和17.9 GHz处出现两个极大反射损耗, 分别为−13.17 dB和−15.36 dB, $Co_{0.7}Cr_{0.1}$-$Zn_{0.2}Fe_2O_4$的极大反射损耗为−8.2和−8.1 dB。PANI-$Co_{0.7}Cr_{0.1}Zn_{0.2}Fe_2O_4$复合材料的反射损耗明显高于铁氧体, 有利于展宽频带[8], 复合材料显示出较好的微波吸收性能。铁氧体反射损耗主要来源于畴壁共振和自旋共振, 以自旋共振为主。聚苯胺反射损耗来源于聚合物中存在的束缚电荷以及对电流的传导性所引起的强烈的极化效应和松弛效应, 铁氧体与聚苯胺复合后相互之间产生了协同作用。复合材料对电磁波的损耗主要由PANI内的双极化效应和极化松弛效应引起的介电损耗和铁氧体自旋共振引起的磁损耗以及聚合物和磁性颗粒界面之间的松弛效应共同决定的[18]。多种因素的叠加, 导致PANI-$Co_{0.7}Cr_{0.1}Zn_{0.2}Fe_2O_4$复合材料的反射损耗明显高于铁氧体。

3 结　论

1. 在$Co_{0.8}Zn_{0.2}Fe_2O_4$铁氧体中掺杂Cr^{3+}离子导致其晶格常数从0.8409 nm减小到0.8377 nm。

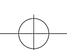
2. PANI-$Co_{0.7}Cr_{0.1}Zn_{0.2}Fe_2O_4$ 复合材料的 M_s, M_r 和 H_c 的数值分别为 8.80 emu·g^{-1}, 3.14 emu·g^{-1} 和 37.22 kA·m^{-1}, 均小于 $Co_{0.7}Cr_{0.1}Zn_{0.2}Fe_2O_4$ 铁氧体的相应数值。

3. PANI-$Co_{0.7}Cr_{0.1}Zn_{0.2}Fe_2O_4$复合材料在14.1 GHz和17.9 GHz处出现两个极大反射损耗, 数值为−13.17 dB和−15.36 dB, 明显高于铁氧体的相应数值, 具有较高的微波吸收性能。

参 考 文 献

1　J. W. Ye, Y. Liu, X. F. Chen, M. Yao, Microwave electromagnetic and absorption properties of Sm N/α-Fe/$Sm_2Fe_{17}N_3$ composites in 0.5-18 GHz range, J. Alloys. Compd., **526**, 59(2012)

2　S. Ke, W. L. Zhong, Y. Zhong, L Li, X. Jiang, H. Ji, Temperature dependence of core losses at high frequency for MnZn ferrites, Physical B, **405**, 1018(2010)



3 WU Yanfei, HUANG Ying, ZHANG Yinling, NIU Lei, Several w-type barium ferrites with different Me_2: preparation and the electromagnetic properties, Chinese Journal of Materials Research, **25**(6), 607(2011)
(吴燕飞, 黄 英, 张银铃, 牛 磊, Me_2-W型钡铁氧体的制备及其电磁性能研究, 材料研究学报, **25**(6), 607(2011))

4 K. Gupta, P. C. Jana, A. K. Meikap, Electrical transport and optical properties of the composite of polyaniline with gold, Solid State Sci, **14**, 324(2012)

5 Y. Yao, H. Y. Jiang, J. Wu, D. Gu, L. Shen, Synthesis of Fe_3O_4/polyaniline nanocomposite in reversed micelle systems and its performance characteristics, Proc. Eng., **27**, 664(2012)

6 LI Yuanxun, LIU Yingli, ZHANG Huaiwu, LING Weiwei, XIE Yunsong, XIAO Johnqiang, Preparation, Characterization and properities of polyaniline-barium ferrite nanocomposite, Chemical Journal of Chinese Universities, **29**(3), 640(2008)
(李元勋, 刘颖力, 张怀武, 凌味未, 谢云松, XIAO JohnQiang, 聚苯胺钡铁氧体纳米复合材料的制备、表征及性能, 高等学校化学学报, **29**(3), 640(2008).)

7 S. P. Gairola, V. Verma, L. Kumar, M. A. Dar, S. Annapoomi, R. K. Kotnala, Enhanced microwave absorption properties in polyaniline and nano-ferrite composite in X-band, Synth. Met., **160**, 2315 (2010)

8 C. C. Yang, Y. J. Gung, W. C. Hung, T. H. Ting, K. H. Wu, Infrared and microwave absorbing properties of $BaTiO_3$/polyaniline and $BaFe_{12}O_{19}$/polyaniline composites, Compos. Sci. Technol., **70**, 466 (2010)

9 R. T. Ma, Y. W. Tian, H. T. Zhao, G. Zhang, H. Zhao, Synthesis, Characterization and electromagnetic studies on nanocrystalline $Co_{0.5}Zn_{0.5}Fe_2O_4$ by polyacrylamide gel, J. Mater. Sci. & Technol., **24**(4), 628(2008)

10 C. C. Hwang, J. S. Tasi, T. H. Huang, Combustion synthesis of Ni–Zn ferrite by using glycine and metal nitrates—investigations of precursor homogeneity, product reproducibility, and reaction mechanism, Mater. Chem. Phys., **93**, 330(2005)

11 C. J. Leng, J. H. Wei, Z. Y. Liu, J. Shi, Influence of imidazolium-based ionic liquids on the performance of polyaniline- $CoFe_2O_4$ nanocomposites, J. Alloys Compd., **509**, 3052(2011)

12 C. D. Prasanna, H. S. Jayanna, A. R. Lamani, S. Dash, Polyaniline/$CoFe_2O_4$ nanocomposites: A novel synthesis, characterization and magnetic properties, Synth. Met., **161**, 2306(2011)

13 D. S. Birajadar, U. N. Debatwal, K. M. Jadhav, X-ray, IR and bulk magnetic properties of $Cu_{1-x}Mn_xFe_{2-2x}O_4$ ferrite system, J. Mater. Sci., **37**, 1443(2002)

14 L. C. Li, J. Jiang, F. Xu, Synthesis and ferromagnetic properities of novel Sm-substituted LiNi ferrite-polyaniline nanocomposite, Mater. Lett., **61**, 1091(2007)

15 G. Namita, S. Kuldeep, O. Anil, D. P. Singh, S. K. Dhawan, Thermal, dielectric and microwave absorption properties of polyaniline-$CoFe_2O_4$ nanocomposites, Compos. Sci. Technol., **71**, 1754(2011)

16 Y. P. Duan, G. L. Wu, X. G. Li, On the correlation between structural characterization and electromagnetic properties of doped polyaniline, Solid State Sci., **12**, 1374(2010)

17 S. W. Phang, T. Hino, M. H. Abdullah, N. Kuramoto, Applications of polyaniline doubly doped with p-toluene sulphonic acid and dichloroacetic acid as microwave absorbing and shielding materials, Mater. Chem. Phys., **104**, 327(2007)

18 T. H. Ting, R. P. Yu, Y. N. Jau, Synthesis and microwave absorption characteristics of polyaniline/NiZn ferrite composites in 2-40 GHz, Mater. Chem. Phys., **126**, 364(2011)

